Electrochemical Investigations
IN THE DEVELOPMENT OF

by **Victoria J. Gelling**,
Akash Saraf,
Niteen Jadhav,
The Valspar
Corporation

Historically, corrosion and coatings research has been a visual, qualitative, and subjective study. ASTM B117 (Standard Test Method of Salt Spray Testing) is one of the most widely used methods in corrosion experiments, and many users visually interpret scribe creepage or blister density. Electrochemical methods offer the pathway towards quantitative corrosion measurements. Electrochemical techniques have been utilized in the past few decades as important methods in the study of corrosion and coating degradation. Electrochemical techniques allow for the determination of changes in material properties, which often occur prior to visual changes and provide information regarding corrosion mechanisms. Indeed, by using these techniques, such as electrochemical impedance spectroscopy (EIS), scanning electrochemical microscopy (SECM), and scanning vibrating electrode technique (SVET), important mechanistic information regarding protection/ failure transitions can be determined.

For this study, three different powder coating systems (a one-coat DTM polyester, a two-coat system with two cure cycles, and a two-coat system with a single cure cycle) were investigated using EIS at both the intact portion (face area) of the coating and the edge of the panel. With EIS analysis, it was found that the DTM coating system exhibits signs of water ingress and the other two systems are unaffected at the face area, whereas better corrosion protection was observed for a two-coat system with two cure cycles and a two-coat system with a single cure cycle, as compared to the one-coat DTM system. Initial studies of the systems utilizing SVET exhibited a barrier type of protection for a two-coat system with two cure cycles. The

most important highlight of this work was the development of an electrochemical screening method for the corrosion prediction on the panel edges.

INTRODUCTION

In recent years, electrochemical assessment of coatings has provided significant insight into the mechanisms of both corrosion protection and, correspondingly, the failure of coatings. However, at this time, the techniques have not been universally used in industrial coating research. Understanding the localized beginnings of corrosion events via electrochemical techniques will not only allow for appropriate coating design parameters, but could also be used as predictive modeling methods for coating lifetimes.

Upon review of the literature, it is apparent that very little study has been conducted on utilizing electrochemical techniques to determine the relationship between compositional and structural variations in polymeric coatings and their corrosion-protective properties. In the few papers found on the topic, interesting results were observed indicating significant insight into structure–property relations. Lobnig et al. determined that EIS was an effective tool to determine critical pigment volume concentrations (CPVC).[1] Correspondingly, it is also possible to determine, by localized EIS (LEIS), the uniformity of the dispersion of pigment particles.[2] The influence of pigment size and shape on the resulting corrosion inhibition of steel has been studied by joining EIS with microscopy techniques.[3] Duval et al. studied the influence of polymer structure on the corresponding organic coatings in sour media; however, the scope of the project was extremely focused with regard to the polymer structures, substrate, and corrosive environments.[4] A more recent study by Upadhyay et al.
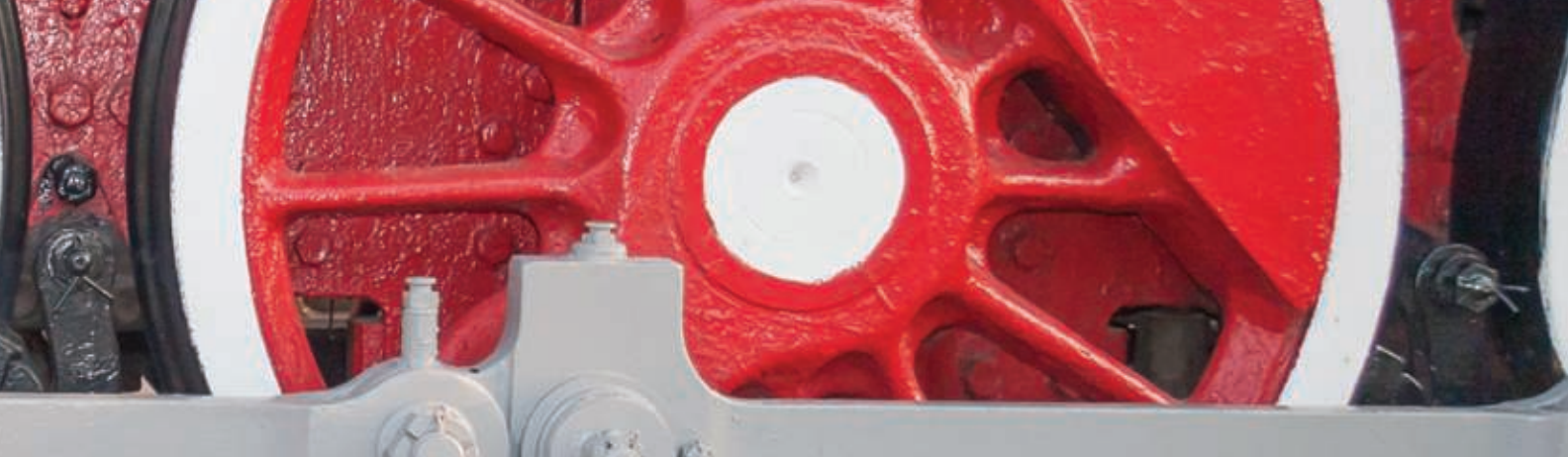
High Performance Coatings

demonstrated that systematic variations in coatings binder chemistry could be clearly reflected in EIS measurements.[5]

EIS is a nondestructive evaluation technique that is commonly used on coated metallic substrates. By measuring the current, voltage, and phase shift between the two, impedance *(Z)* can be calculated where *V* is the voltage applied, *I* is the current measured, and *Z* is the resulting impedance, which are all functions of the applied frequency. A known voltage is applied between the working and reference electrodes, and the resulting current is measured between the working and counter electrode while the frequency of the voltage is swept from high to low. A small AC perturbation about the open circuit potential reduces the risk of causing any degradation to the measured sample and, hopefully, maintains the sample at steady-state.

Superior barrier coatings tend to have a completely capacitive response over the measured frequency range with a high (> 10^9 ohms) impedance upon initial exposure.[6] With increased exposure to an electrolyte, the impedance will decrease with time until corrosion occurs, which then drastically reduces the low frequency impedance. The onset of corrosion is typically signified with the development of a secondary half circle on the Nyquist plot. From the EIS graphs in *Figure* 1, it can be determined whether that sample is displaying a capacitive behavior, a Randles cell behavior, or localized failure behavior. Many other behaviors are also possible.[7] Certainly, some of the changes determined by EIS are due to water ingress. Therefore, it is possible to study the plasticizing influence of water on the coatings, which can significantly decrease the glass transition temperature (T_g) of the coating.[6] Thus, it is possible to perform EIS on the coatings as temperature is changed to determine the changes in T_g related to water uptake and how the changes in T_g influence the protection provided to the substrate.[8]

In comparison with EIS measurements, SVET is a more recent experimental method and is finding a multitude of uses in the study of corrosion, metals, and material degradation. This in-situ, local technique utilizes a conductive probe which measures the variation in voltages, created via the small current dipoles, by vibrating on multiple axes and referencing a probe far from the sample surface.[7] Measuring the voltage difference and knowing the amplitude of vibration along with the resistivity of the solution leaves a simple equation for determining the current at that location. The current is a quantitative measurement of the corrosion rate for the sample when exposed to the immersion electrolyte.

Powder coatings are solvent-free, 100% solid coating systems that have been used as zero- or low-VOC alternatives to conventional liquid coatings. Unlike liquid coatings, powder coating systems typically yield greater than 95% material usage, thereby providing lower applied cost. Traditionally, single-coat powder systems [direct-to-metal (DTM)] have dominated the marketplace. It is difficult, however, to adequately protect certain parts of a metal substrate, including edges and corners. Consequently, edge corrosion is a common problem. To combat edge corrosion, a low-flow coating which provides good edge coverage is used. However, such coatings have a tendency to produce wavy surfaces characterized as orange peel. On the other hand, when flow is increased to provide greater smoothness, edge coverage thins, and may fail altogether, leaving metal parts prone to edge corrosion. Conventional systems that attempt to combine flow characteristics with increased surface smoothness typically require multiple application and heating steps, leading to process inefficiency and delay. However, as perfor-
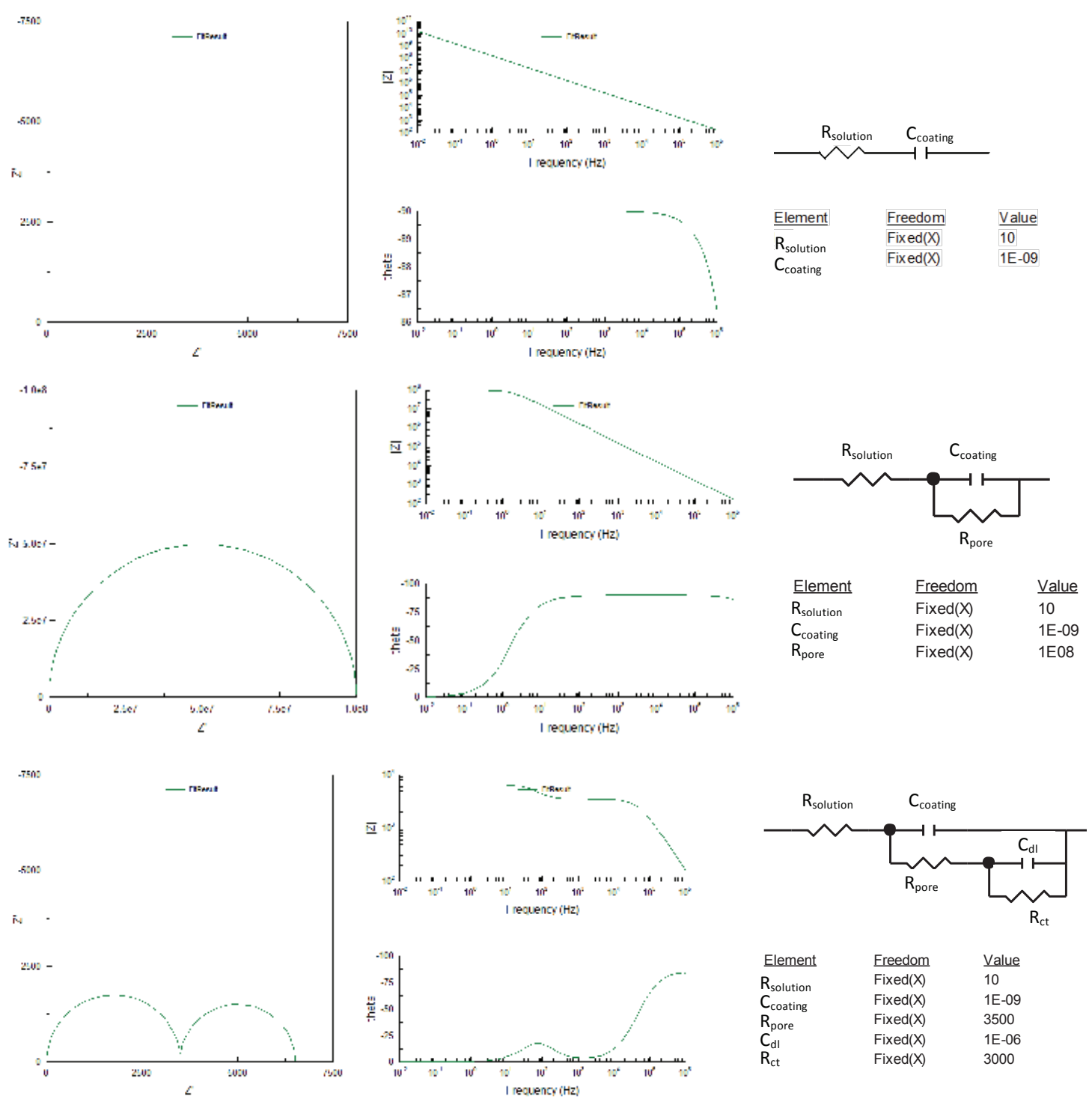
Figure 1—Impedance schematic for a perfect coating (top), a typical coating (middle), and a failing coating (bottom). The graphs are drawn from ZView® software, by Scribner Associates, Inc.

Table 1—Coating Systems with Acronyms[a]

Acronym	DTM	2C2B	2C1B
Coating system	DTM Polyester (1-Coat, 1-Bake)	Hybrid Primer Polyester topcoat (2-Coat, 2-Bake)	Polyester Primer Polyester topcoat (2-Coat, 1-Bake)
Coating details	**Film Thickness** 70-90 microns **Cure Condition** 10 min 205°C	**Hybrid Primer** **Film Thickness** 35-50 microns **Cure Condition** 10 min 205°C **Polyester Topcoat** **Film Thickness** 35-50 microns **Cure Condition** 10 min 205°C	**Polyester Primer** Film thickness 35-50 microns **Polyester Topcoat** **Film Thickness** 35-50 microns **Cure Condition** 10 min 205°C

(a) Cure temperatures listed are peak metal temperatures.

mance and corrosion specifications are becoming increasingly stringent in general, industrial market-space multicoat coating systems are starting to become more popular.

For this study, three different powder coating systems were investigated using EIS at both the intact portion of the coating and the edge. The three systems were a one-coat DTM polyester, a two-coat system with two cure cycles, and a two-coat system with a single cure cycle. Additionally, preliminary studies of the systems utilizing SVET have begun to determine the corrosion protection afforded to an active metal substrate.

EXPERIMENTAL

The aforementioned coatings were applied on cold rolled steel (CRS) laser-cut window panels with dimensions of 100 x 200 x 3.2 mm. These panels were iron-phosphate pretreated and rinsed with deionized water before the powder coating application. For SVET analysis, a 10 x 10 mm square was cut out of an ACT cold rolled steel panel with dimensions of 100 x 200 x 1 mm, which was iron-phosphate pretreated and washed with deionized water before the application of the powder coating. The three systems used in this study are described in *Table 1*, along with acronyms and detailed information on the different coating systems.

Gamry Instruments R600 Potentiostat/ Galvanostat/ZRA with Gamry Framework Version 5.58/EIS 300 software was employed for EIS measurements. EIS was performed with a three-electrode setup which included the coated substrate as a working electrode, platinum mesh as a counter electrode, and silver–silver chloride as a reference electrode. EIS data for edge corrosion measurement was collected at 5 mV perturbation voltage and, for flat panel data, was collected at 10 mV perturbation voltage. Data was collected at 10 points/ decade over the frequency range of 100,000 to 0.01 Hz. Panels were under constant immersion in Dilute Harrisons solution (DHS, 0.35 wt% ammonium sulfate + 0.05 wt% sodium chloride) and were removed at regular intervals for EIS measurements. DHS was also used as an electrolyte for the EIS measurements. The measurements were taken at initial, 7 day, 15 day, and 25 day intervals. All EIS measurements were performed with five replicate samples, with representative results shown in this article. Raw impedance values are used throughout this work. For the face EIS measurements, the surface area measured was approximately 13.85 cm^2. For the edge measurements, the surface area is unknown, but was constant for all samples.

SVET from Applicable Electronics, Inc. was used for current density measurements. A Pt–Ir microelectrode was coated with platinum black on its tip and was employed as a vibrating probe. DHS media was used for the SVET measurements. An artificial defect was created using a razor blade at the center of the coating and was immersed in DHS. Data was collected with a vibrating probe as close as 150 μm to the surface. Data was plotted with positive current as anodic current and negative current as cathodic current in Origin® software.

Figure 2—(a) A typical three-electrode EIS electrochemical cell for coatings on metal substrates and (b) a window panel for edge EIS measurement.
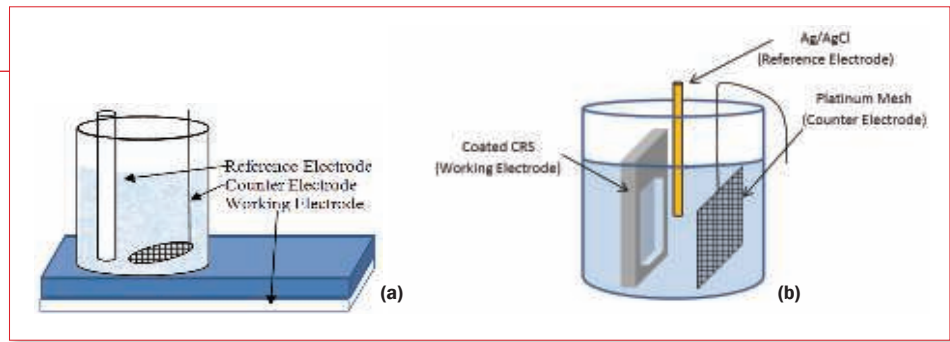
Figure 3—Bode plot for the (a) face measurement of the samples and (b) the edge measurement.
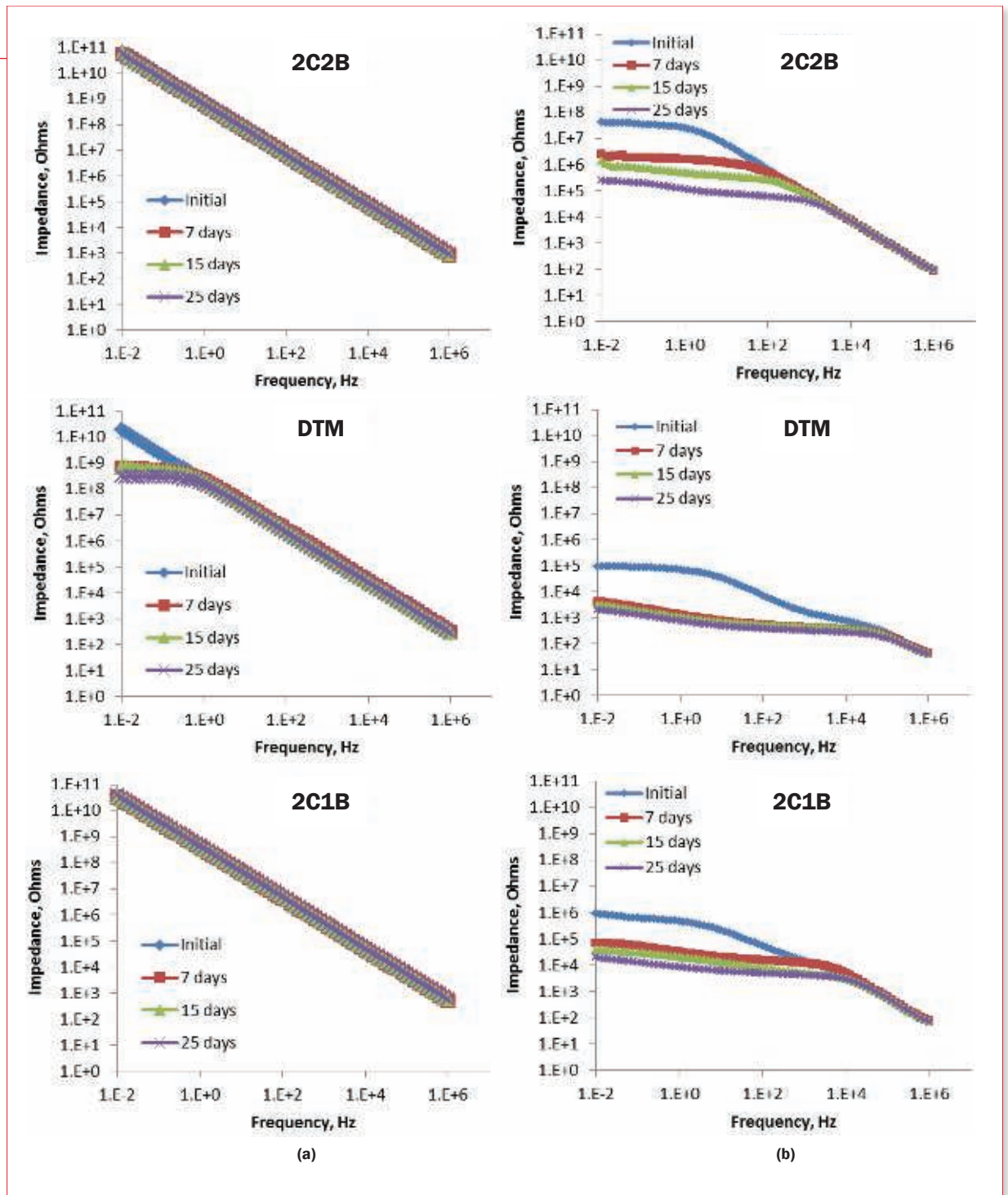
RESULTS AND DISCUSSION

EIS on Face of the Coated Substrate

To perform the EIS experiment on an adhered "face" of a coated sample, a three-electrode electrochemical cell was adhered to the coated substrate, as shown in *Figure* 2a. For this study, in addition to measuring the EIS on the face of the coated specimen, edge measurements were also conducted. To perform the edge measurement, a window sample (*Figure* 2b) was immersed into the DHS with subsequent EIS measurement using the standard counter and reference electrodes, as described in the Experimental section of this article. It should be noted that, in this case, the surface area for the edge measurement is significantly higher than that of the face measurement result detailed in the prior section. Therefore, throughout this study, raw impedances are provided.

As shown in *Figure* 3a, all three systems displayed very high impedance, approximately 10^{11} ohms at low frequency (0.01 Hz). Additionally, the initial results for all three systems appeared to be very capacitive in nature, as indicated by the linear, decreasing impedance with increasing frequency. The capacitive nature of the coating, which is indicative of a perfect barrier, was observed for both 2C2B and 2C1B for 25 days of constant immersion in DHS. The DTM sample, however, did display decreases in low frequency impedance after only seven days of immersion in DHS. Additionally, this decrease in low frequency impedance is reflected in the change of circuit model from that of *Figure* 1 (top) to *Figure* 1 (middle) as the resistive component was evident in the Bode plot after seven days of immersion in DHS. Low frequency impedance (0.01 Hz) continued to decrease to approximately 10^8–10^9 ohms after 25 days of constant immersion in DHS. Even though a coating resistive element was observed after the immersion of the DTM sample, the impedance values are still indicative of good barrier properties.[9] While improved barrier properties were exhibited by 2C2B and 2C1B during the brief immersion in DHS presented in this study in comparison to the DTM sample, there was insufficient immersion time to differentiate the 2C2B and 2C1B coatings.

As corrosion often commences from inherent defects or edges of samples, the samples were studied further. To better characterize the protection provided by the three-coating systems, EIS was performed in such a manner as to elucidate the barrier properties and impedance response of the coating on the edges of the samples, with results shown in the following section.

EIS on Edge of the Coated Substrate

The edge area tends to be the weakest area on any surface, often due to the natural thinning of the coating in those areas and/or due to inherent stresses which can occur. These weaknesses often dictate when corrosion can occur. It will show its first signs at the edges, and will inevitably result in the failure of the paint. Panels on which the face was measured, as in the previous section, were used in this study for characterizing the edge protection.

As observed in *Figure* 3b, and as expected, all three systems displayed a decrease in low frequency impedance as compared to the face measurements shown in *Figure* 3a, most likely due to a slight decrease in coating thickness. Additionally, all samples exhibited changes within seven days of immersion in DHS, signifying the decreased protection provided at the edges in comparison to the face of the samples. Interestingly, and importantly, samples 2C2B and 2C1B displayed one to two orders of increase in low frequency impedance, and therefore had superior barrier protection of the edge in comparison with the DTM sample. There may be a slight increase in protection, initially, provided by the 2C2B sample in comparison with the 2C1B sample. However, after 25 days of immersion, both systems still outperformed the DTM sample. After seven days of immersion, the DTM sample provided little, if any, protection to the edge as the low frequency impedance had decreased to a value very similar to that of the uncoated substrate (i.e., the charge transfer resistance) while at the same time the resistance of the coating was almost negligible, as the coating was severely damaged from the rampant corrosion.

One important finding in the study was that while 25 days of immersion was insufficient time to differentiate between the 2C2B and 2C1B samples, significant differences were determined by the edge technique. After only 30 minutes of exposure to DHS, followed by a 30-minute EIS experiment, the electrochemical technique was able to determine the increased protection provided by the 2C2B coating to the edge of the window substrate.

Circuit Modeling of the EIS Results

The EIS data for both the face and edge measurements was fitted to equivalent circuits. However, due to the lack of significant changes in the 2C2B and 2C1B samples, the focus of this section is the results obtained from the edges. Circuit models used are shown in *Figure* 4 and respective electrical components were extracted for both the face and edge measurements and are represented in the *Appendix*.

**Figure 4**—Equivalent circuit models employed for EIS data fitting.
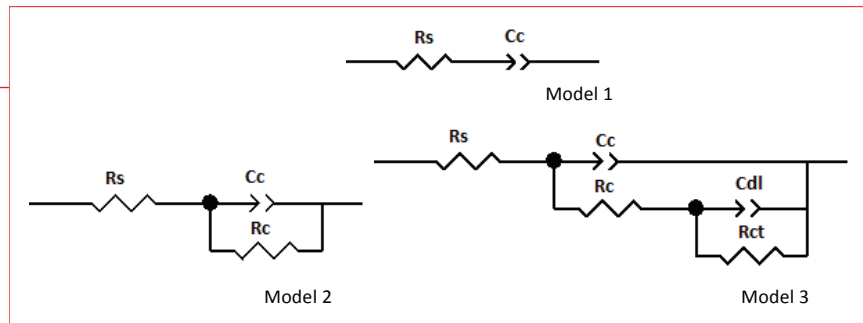
Model 1 (*Figure* 4) was used for 2C2B face, 2C1B face, and DTM (initial) face measurements, due to the extremely high barrier properties of the coating. Model 2 (*Figure* 4) was used for DTM face (7, 15, and 25 day measurements), and 2C2B edge measurements. Model 3 (*Figure* 4) was used for DTM edge and 2C1B edge measurements. In the models, Rs is the solution resistance, Cc is the coating capacitance extracted for the constant phase element associated with the coating, Rc is the coating resistance, Cdl is the double layer capacitance associated with the coating/metal interface extracted for the second constant phase element, and Rct is the charge transfer resistance associated with the coating/metal interface. Exponent "P" represents whether is coating is purely capacitive (P=1) or purely resistive (P=0). Value of "P" between 0 and 1 represents the mixed nature of the coating. With high barrier properties, Rc becomes beyond the instrument's capabilities to measure and only the coating capacitance is observed (Model 1).

Overall, the results indicate the improvement in barrier protection provided with both of the two-coat systems, 2C2B and 2C1B, in comparison with the one-coat DTM sample. Additionally, no negative influence of the one-bake cure condition was observed for the coating on the face of the sample, as the 2C2B and 2C1B samples performed equally, as determined by the high, unchanging barrier properties (see *Figure* 5a). Due to the high barrier properties and capacitive nature of the 2C2B and 2C1B coatings throughout the immersion time, as well as the initial measurement of the DTM sample, the boxed data points in *Figure* 5a should be taken to mean that the coating resistance, Rc, is greater than 1×10^{11} ohms, which is beyond the instrumental capabilities to measure.

The Rc was highest for 2C2B coating, followed by the 2C1B. Both two-coat systems outperformed the DTM coatings, offering significantly better barrier protection at the edge (*Figure* 5b). A second time constant was apparent for both the DTM and 2C1B coating, which may be attributed to the corrosion reaction occurring at the coating metal interface. Rct represents the resistance to the corrosion reaction at the coating/metal interface, which was higher for 2C1B coating as compared to DTM coating, which indicated better corrosion protection
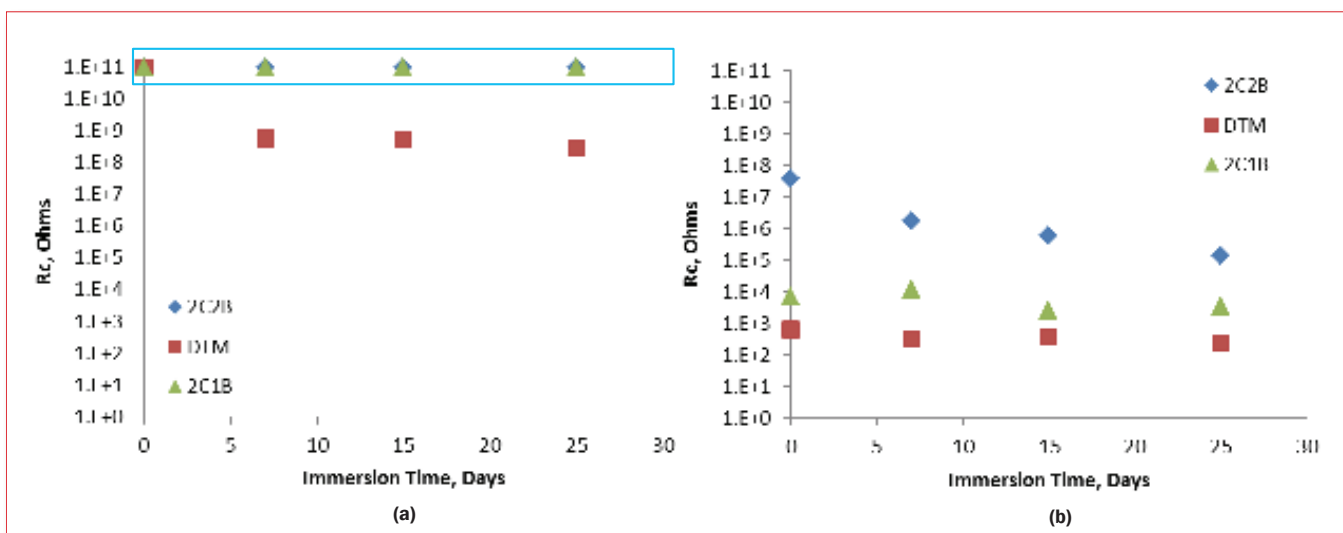
Figure 5—Changes in Rc with immersion time in DHS: (a) face and (b) edge.
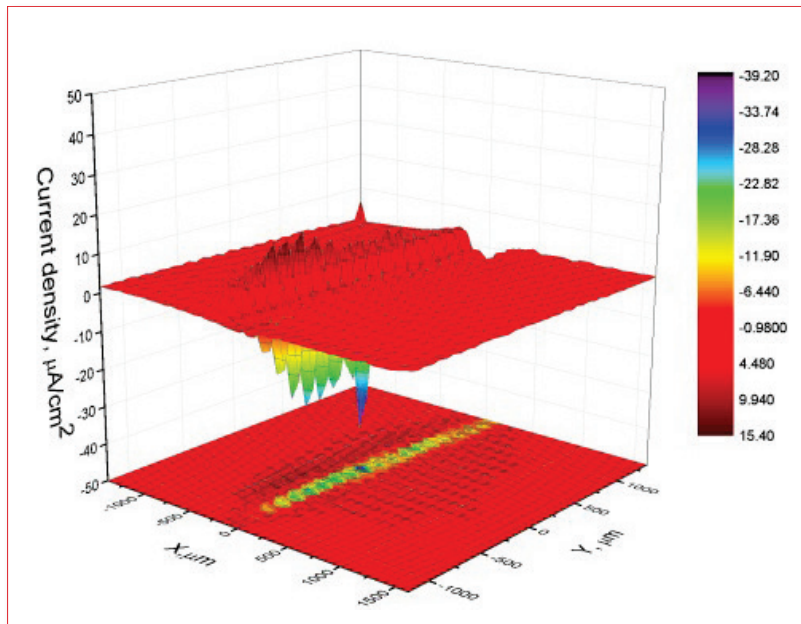
Figure 6—SVET current density map for 2C2B coating after six hours of immersion in DHS.

at the edge for the 2C1B coating as compared to DTM coating. Visual inspection revealed significant corrosion for the DTM sample, approaching 100% of the edge. In comparison, the 2C1B sample had less than 25% of the edge affected and the 2C2B coating had no visual changes at all.

Preliminary Scanning Vibrating Electrode Technique

At the time of writing this article, the SVET research was just at the preliminary stage. An early example of the results obtained for a 2C2B coating with artificial defect, after six hours of immersion in DHS, is provided in *Figure* 6, where both anodic (oxidation) and cathodic (reduction) current is primarily confined to the defect area.[7]

This result indicates that while corrosion can commence at an induced defect, no inherent defects were present that allowed for other measurable anodic or cathodic reactions to occur. This is a testament to the uniform, protective coatings that can be achieved when utilizing powder coatings as a protective layer for active metal substrates. Future studies will be conducted to further probe the mechanisms of protection provided by the 2C2B system in comparison to the 2C1B and DTM systems.

CONCLUSIONS

From the EIS results, very few, if any, differences were observed for the EIS response for the face surfaces of the 2C2B and 2C1B systems; however, the DTM sample did display signs of electro-chemical changes, possibly signifying slight water ingress into the coating. It is evident that 2C2B and 2C1B coatings exhibited better protection at the edges when compared to DTM coatings. This suggests that a two-coat system (2C2B and 2C1B) provides an increase in protection over mono-coat systems (such as DTM sample). Additionally, there may be further benefits to curing the primer prior to the topcoat application. However, the 2C1B system matches the performance of 2C2B system, especially on the face of the substrate, eliminating the need for additional cure of the primer and thereby reducing energy consumption by half. Results further demonstrate that EIS can be effectively used for studying corrosion and barrier properties at the edges and corners of powder coated substrates. The SVET measurements showed the presence of both cathodic and anodic currents in the scribe, suggesting the barrier nature of the intact coating for the 2C2B system. ⓒⓣ

References

1. Lobnig, R., Villalba, W., Goll, K., Vogelsang, J., Winkels, I., Schmidt, R., Zanger, R., and Soetemann, J., "Development of a New Experimental Method to Determine Critical Pigment-Volume-Concentrations Using Impedance Spectroscopy," *Prog. Org. Coat., 55* (4), 363-374 (2006).

2. Taylor, S.R., "Incentives for Using Local Electrochemical Impedance Methods in the Investigation of Organic Coatings," *Prog. Org. Coat., 43* (1–3), 141-148 (2001).

3. Vilche, J., Bucharsky, E., and Giudice, C., "Application of EIS and SEM to Evaluate the Influence of Pigment Shape and Content in ZRP Formulations on the Corrosion Prevention of Naval Steel," *Corros. Sci., 44* (6), 1287-1309 (2002).

4. Duval, S., Camberlin, Y., Glotin, M., Keddam, M., Ropital, F., and Takenouti, H., "Characterisation of Organic Coatings in Sour Media and Influence of Polymer Structure on Corrosion Performance," *Prog. Org. Coat., 39* (1), 15-22 (2000).

5. Upadhyay, V., Harkal, U., Webster, D., and Bierwagen, G., "Preliminary Investigation of the Impact of Polymer Composition on Electrochemical Properties of Coatings as Determined by Electrochemical Impedance Spectroscopy," *J. Coat. Technol. Res., 10* (6), 865-878 (2013).

6. Bierwagen, G., Tallman, D., Li, J., He, L., and Jeffcoate, C., "EIS Studies of Coated Metals in Accelerated Exposure," *Prog. Org. Coat., 46* (2), 149-158 (2003).

7. Jadhav, N., Vetter, C.A., and Gelling, V.J., "The Effect of Polymer Morphology on the Performance of a Corrosion Inhibiting Polypyrrole/Aluminum Flake Composite Pigment," *Electrochim. Acta, 102* (0), 28-43 (2013).

8. Li, J., Jeffcoate, C.S., Bierwagen, G.P., Mills, D.J., and Tallman, D.E., "Thermal Transition Effects and Electrochemical Properties in Organic Coatings: Part 1—Initial Studies on Corrosion Protective Organic Coatings," *Corros., 54* (10), 763-771 (1998).

9. Scully, J., Silverman, D., and Kendig, M., *Electrochemical Impedance: Analysis and Interpretation*, ASTM International: West Conshohocken, PA, 1993.

AUTHORS

Victoria J. Gelling, **Akash Saraf**, and **Niteen Jadhav**, The Valspar Corporation, 312 South 11th Ave., Minneapolis MN 55415; Victoria.Gelling@valspar.com.

APPENDIX: Circuit Elements Obtained Through EIS Data

	Time	R_c (Ω)	CPE$_c$ T (F)	CPE$_c$ P	R_{ct} (Ω)	CPE$_{dl}$ T (F)	CPE$_{dl}$ P
2C2B edge	Initial	3.52×10^7	3.04×10^{-9}	0.97	-	-	-
	7 days	1.66×10^6	4.04×10^{-9}	0.95	-	-	-
	15 days	5.99×10^5	5.19×10^{-9}	0.93	-	-	-
	25 days	1.33×10^5	1.06×10^{-8}	0.88	-	-	-
DTM edge	Initial	6.53×10^2	8.73×10^{-9}	0.96	8.33×10^4	1.23×10^{-6}	0.79
	7 days	3.06×10^2	7.96×10^{-9}	0.97	1.25×10^4	5.08×10^{-4}	0.35
	15 days	3.67×10^2	1.34×10^{-8}	0.94	6.31×10^3	6.92×10^{-4}	0.37
	25 days	2.39×10^2	9.84×10^{-9}	0.96	4.21×10^3	9.40×10^{-4}	0.33
2C1B edge	Initial	6.65×10^3	3.31×10^{-9}	0.98	6.25×10^5	2.61×10^{-7}	0.65
	7 days	1.14×10^4	3.67×10^{-9}	0.98	8.24×10^4	1.76×10^{-5}	0.41
	15 days	2.45×10^3	2.63×10^{-9}	1	5.13×10^4	2.24×10^{-5}	0.31
	25 days	3.36×10^3	3.38×10^{-9}	0.99	4.05×10^4	9.66×10^{-4}	0.29
2C2B face	Initial	$>1 \times 10^{11}$	2.19×10^{-10}	0.99	-	-	-
	7 days	$>1 \times 10^{11}$	2.71×10^{-10}	0.98	-	-	-
	15 days	$>1 \times 10^{11}$	2.55×10^{-10}	0.98	-	-	-
	25 days	$>1 \times 10^{11}$	2.72×10^{-10}	0.97	-	-	-
DTM face	Initial	$>1 \times 10^{11}$	7.98×10^{-10}	0.98	-	-	-
	7 days	5.61×10^8	7.24×10^{-10}	0.98	-	-	-
	15 days	5.49×10^8	7.50×10^{-10}	0.98	-	-	-
	25 days	2.96×10^8	8.92×10^{-10}	0.97	-	-	-
2C1B face	Initial	$>1 \times 10^{11}$	3.76×10^{-10}	0.98	-	-	-
	7 days	$>1 \times 10^{11}$	4.24×10^{-10}	0.98	-	-	-
	15 days	$>1 \times 10^{11}$	3.87×10^{-10}	0.98	-	-	-
	25 days	$>1 \times 10^{11}$	3.85×10^{-10}	0.98	-	-	-